

Investigation of the three-dimensional ruthenium distribution in fresh and aged membrane electrode assemblies with synchrotron X-ray absorption edge tomography

Tobias Arlt¹, Ingo Manke¹, Klaus Wippermann², Christian Tötzke¹, Henning Markötter¹, Heinrich Riesemeier³, Jürgen Mergel², John Banhart¹

¹) Helmholtz-Zentrum Berlin, Hahn-Meitner-Platz 1, 14109 Berlin

²) Forschungszentrum Jülich, 52425 Jülich

³) BAM, Bundesanstalt für Materialforschung und -prüfung, Unter den Eichen 87, 12205 Berlin

Keywords

Edge tomography; ruthenium distribution; direct methanol fuel cells; synchrotron X-ray; PtRu corrosion.

Abstract

Synchrotron X-ray absorption edge imaging was used to investigate the ruthenium distribution in both fresh and aged Pt/Ru-based membrane electrode assemblies (MEA) of direct methanol fuel cells. MEAs aged in different ways were analyzed: artificially aged by MeOH depletion and aged for 1700 h in an operating fuel cell stack. An element sensitive tomographic technique – differential X-ray absorption edge tomography – was applied allowing for a 3D-visualization of the ruthenium distribution within the MEA. We found a markedly changed Ru distribution after aging which is correlated to the GDL structure, the flow field geometry, and CO₂ transport in the methanol solution.

1. Introduction

Fuel cells are expected to play an important role in the energy management of both mobile (cars, trucks etc.) and stationary (industry, power plants) facilities [1]. Direct methanol fuel cells (DMFC) use air and diluted methanol as reactants at the cathode and anode side, respectively. As they are operated at temperatures of only up to about 70 °C they belong to the category of low temperature cells.

Aging of the component materials is one of the key issues for the development of durable fuel cells. For DMFCs, ruthenium corrosion limits long-term stability [2] [3] [4] [5]. The mechanism of Ru corrosion, the nature of the corrosion and their transport behavior within the

cell is not well understood. Detailed knowledge of aging mechanisms is essential to identify appropriate operation conditions, to ensure minimum deterioration and to develop cell components and cell design with respect to an optimal long-time performance. As known, aging effects are highly influenced by transport processes inside the cell components, especially by fluid/gas transport processes in the gas diffusion layers (GDLs), membrane and flow field channels.

There are many reports about XANES (X-Ray Absorption Near Edge Spectroscopy) studies on catalysts [6]. However the technique lacks in spatial resolution. On the other hand, synchrotron X-ray radiography and tomography are powerful techniques for spatially resolved in-situ investigations on operating fuel cells and ex-situ analysis of gas diffusion layers[7] [8] [9].

In this paper, we report on ex-situ investigations of the distributions of ruthenium (Ru) in aged MEAs by means of synchrotron X-ray absorption edge tomography. Compared to conventional absorption contrast tomography at arbitrary energies this technique provides much higher element sensitivity.

2. Experimental set-up

The measurements were performed at the tomography station located at the electron storage ring BESSY (BAMline, Helmholtz-Zentrum Berlin, Germany). For image acquisition, a PCO 4000 camera with a total resolution of 4008×2672 pixels was used. The used pixel size was about $2.1 \mu\text{m}$. A single tomogram comprised 1500 radiographic projections covering an angle range of 180° .

3. Sample preparation

On the anode side, the MEA contained carbon-black supported platinum / ruthenium catalyst produced by Johnson Matthey (HiSpec 12100) with a Pt-Ru loading of 2 mgcm^{-2} . On the cathode side, a carbon-black supported platinum catalyst (Johnson Matthey HiSPEC9100) was used with a Pt loading of also 2 mgcm^{-2} . A Nafion-115 polymer membrane (Dupont) served as membrane.

The first investigated sample was an “artificially” aged MEA subjected to an accelerated aging procedure of methanol depletion. Therefore, the MEA was operated at a temperature of $70 \text{ }^\circ\text{C}$ and a current density of 250 mAcm^{-2} . The anode was supplied with 1 M methanol solution while air was fed to the cathode with a stoichiometry of $\lambda_{\text{methanol}} = \lambda_{\text{air}} = 4$. In the subsequent step, the methanol supply was stopped for 400 s . As a result, fuel depletion occurred in the anode and the process of methanol oxidation could no longer maintain the

electrical current. Instead, water oxidation took place generating oxygen and protons. This process led to a sharp increase in anode potential up to more than 1.2 V / SHE and a reversal of the cell voltage (“cell reversal”). The high anode potential gave rise to corrosion of the anode catalyst, especially of ruthenium, as well as corrosion of the carbon black support. In this experiment, a cell voltage of -2 V was achieved after 400 s. The methanol feed was immediately started again. After this accelerated aging test, the MEA was irreversibly damaged.

The second type of MEA investigated was a specimen long-term aged in a fuel cell stack. The stack had been running for approximately 1700 h at different operating conditions which were appropriately adjusted to avoid irreversible damage on the cell components. Throughout the aging process, single cell voltages never fell below 200 mV which excluded cell reversal due to methanol depletion.

The specimen in the following denoted as “fresh” refers to an unused sample.

4. Differential X-ray edge imaging

Fig. 1a shows a synchrotron X-ray tomogram of a part of a fresh MEA with a diameter of about 3 mm. The GDL structure, consisting of regularly ordered fiber bundles with a periodicity of 1 mm, is clearly visible. The catalyst particles on both sides are displayed in red, most of them are hidden behind the GDL. It is almost impossible to distinguish between Pt and Ru or small amounts of Ru and C in the GDL, respectively.

Differential X-ray K-edge tomography was applied to extract the Ru from the Pt and C distribution. For this purpose, two tomograms close to the X-ray K-edge of Ru at 22.127 keV were taken: One tomogram below the edge at 21.7 keV and the other one above at 22.5 keV.

Owing to electron excitations in the K-shell the transmission of Ru at 22.5 keV is strongly decreased compared to the transmission at 22.127 keV. In contrast, the attenuation of all other material components (C and Pt) decrease or remain almost constant.

In the quotient of both tomograms, i.e. the tomogram taken at 21.7 keV divided by the tomogram at 22.5 keV, all materials except Ru have values of (below or) close to 1, regions with large Ru densities values larger than 1. These regions can be separated from the other parts of the materials. Finally, one of the initial tomograms, e.g. the one at 22.5 keV, can be overlaid on the Ru distribution tomogram as demonstrated in Fig. 1c-e, where Ru is shown in red, while all other materials are shown half-transparent in gray. By producing such composite tomograms, areas with an increased Ru concentration can be correlated with specific features of the GDL.

This procedure was used to analyze the Ru distribution in the fresh, the artificially aged, and the long-term aged MEA.

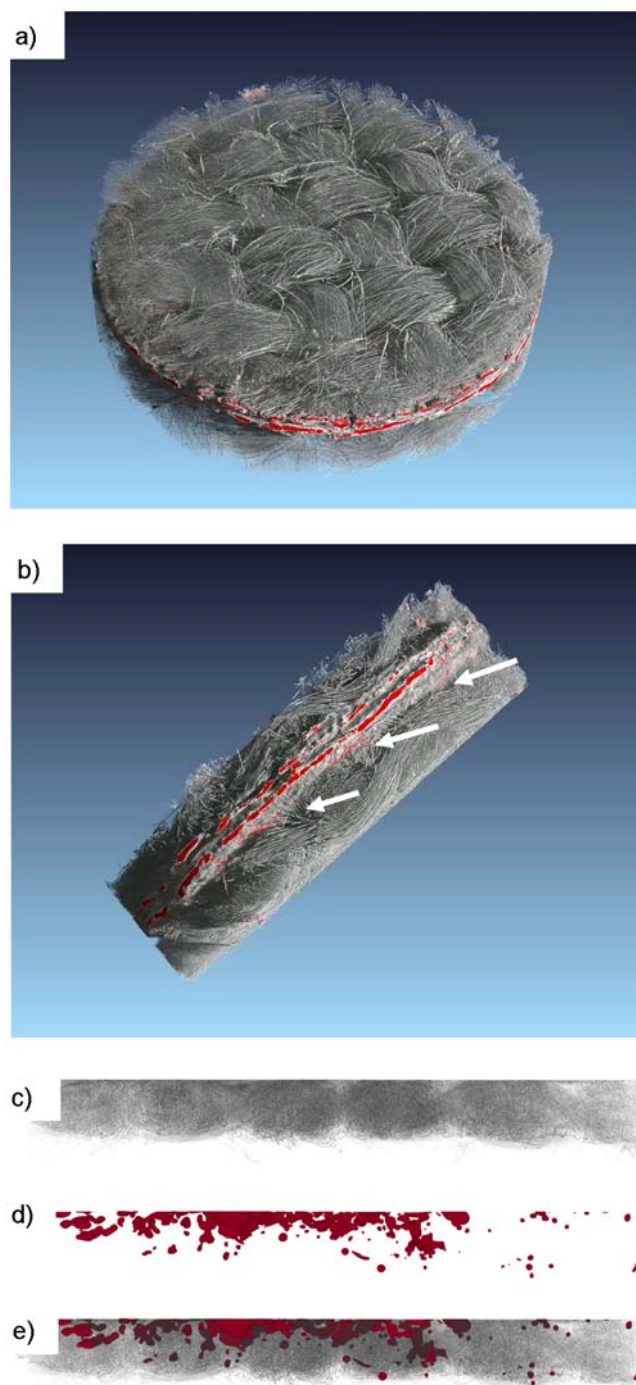


Fig. 1

5. Influence of the GDL structure and channel characteristics

Figs. 2a) and c) show two cross sections through the composite tomogram on both the anode side (a) and cathode side (c) of a fresh MEA. The planes of the cross sections are parallel to and about 50 μm above/below the catalyst layer. Hardly any Ru can be found.

Two corresponding cross sections through anode and cathode are given in Figs. 2b) and d) for the artificially aged MEA. A clear difference was found. In the cross section view of the

cathode (Fig. 2d), again, hardly any Ru could be found, i.e. no changes in the Ru distribution during aging occurred. The cross section through the anode part (Fig. 2b) clearly shows a large amount of Ru that is located inside the GDL. Furthermore, the Ru distribution forms a pattern with the same periodicity as the GDL structure. The ruthenium agglomerates preferably in the free pore space between the woven carbon fibers, especially beneath the membrane. For illustration, these pores are marked by white arrows in Fig. 1b. They originate from the gaps between the fiber bundles in the GDL. The location of these gaps fit well with the observed Ru agglomerates in the GDL.

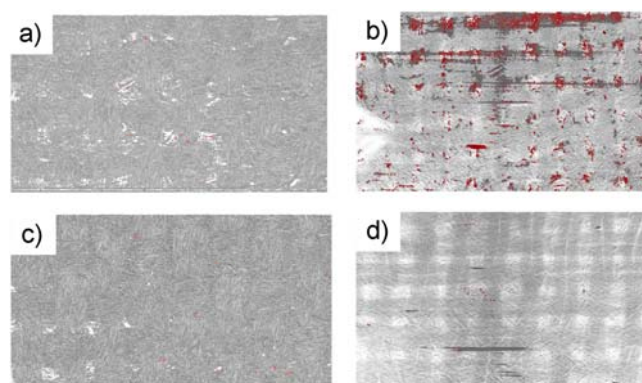


Fig. 2

In next example, the long-term aged MEA was investigated. Fig. 3 shows the Ru distribution in red and all other components (i.e. mainly GDL fibers) in gray. The images show a cross section perpendicular to the membrane plane. In similarity to the artificially aged MEA, strong Ru agglomerates were found on the anode side of the MEA. Again, Ru accumulated preferably in the large pores in between the fiber bundles. The vertical cross section through the membrane (see Fig. 3b) reveals that Ru migrated as much as 50-200 μm deep into the GDL structure and possibly even into the channels.

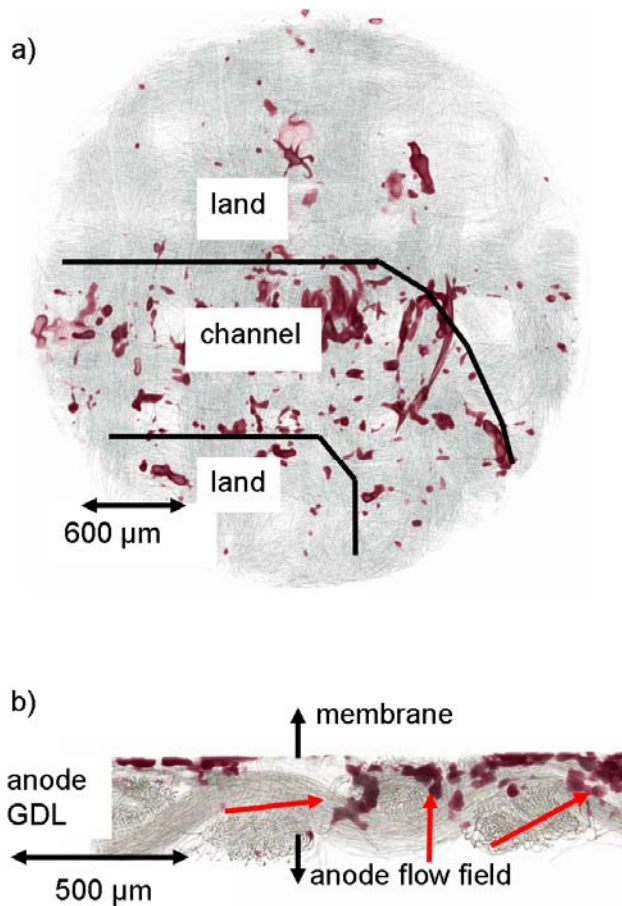


Fig. 3

For the long-term aged MEA, a pronounced correlation between the former flow field characteristics, the fiber structure and the ruthenium distribution was found. More specifically, the amount of Ru is strongly increased along the flow field channel, the margins which are marked by black lines in Fig. 3a. As seen in Fig. 3b, the Ru agglomerates are concentrated closer to the membrane than to the flow field side of the GDL. In contrast, no impact of the former flow field geometry was detected within the artificially aged GDL (Fig. 2c and d), where the Ru agglomerates were found in pores scattered over the entire MEA without a superior adjustment resulting of the flow field.

6. Discussion

The chemical bonds of Ru can be disconnected at high potentials vs RHE [2] so that the Ru can be stripped of the black carbon support and form PtRu alloys, become oxidized or cross over to the cathode side. This disconnection allows diffusion processes, for example through the membrane, and transport processes into the GDL. From previous studies it is known that the pores in between the fiber bundles provide transport paths for the CO₂ gas formed at the catalyst (see Fig. 1b) [7]. Thus it appears likely that the dissolved Ru is transported by means

of carbon dioxide/methanol transport processes through the GDL towards the flow field. This leads to strong Ru agglomerates along the transport paths and beneath the channels in the long-term aged MEA.

In case of the artificially aged MEA, large Ru agglomerates are found inside the pores (indicated by arrows in Fig. 1b), but almost no influence of the flow field channels could be observed. Furthermore the agglomerates in the GDL pores are located much closer to the catalyst layer as compared to the long-term aged MEA. This can be explained by the very short time of only 30 min needed for artificial aging, a period too short to allow for larger diffusion distances of Ru.

7. Conclusions

We have shown that X-ray edge tomography can be used to reveal the distribution of Ru in aged MEAs of DMFCs. Samples subjected to two different aging procedures were investigated: an “artificially” fast aged MEA suffering from methanol depletion and a MEA aged over 1700 h of operation in a fuel cell stack under realistic conditions. We found a clear correlation between the GDL and the flow field channel structure - on the one hand - and the Ru distribution - on the other hand. It is assumed that the preferred CO₂ (also methanol and water) transport paths through the GDL pores and along the channels are responsible for the spatial distribution of Ru agglomerates within the aged MEA. The applied X-ray edge tomography technique is not restricted to the Ru X-ray edge only, and offers a great potential for future investigations of aging effects as well as for studies of various materials properties of fuel cell and battery components.

Acknowledgements

Funding of the project RuN-PEM (grant number: 03SF0324) by the Federal Ministry of Education and Research (BMBF) is gratefully acknowledged.

References

-
- [1] L. Carrette, K.A. Friedrich, U. Stimming, *Fuel Cells* 1 (2001) 5.
 - [2] P. Piela, C. Eickes, E. Brosha, F. Garzon and P. Zelenay, *J. Electrochem. Soc.* 151 (2004) 2053.
 - [3] W. Chen, G. Sun, Z. Liang, Q. Mao, H. Li, G. Wang, Q. Xin, H. Chang, C. Pak, D. Seung, *J. Power Sources* 160 (2006) 933.
 - [4] T.I. Valdez, S. Firdosy, B.E. Koel, S.R. Narayanan, *ECS Transactions*, 1 (6) (2006) 293.

-
- [5] M.K. Jeon, K.R. Lee, K.S. Oh, D.S. Hong, J.Y. Won, S. Li, S.I. Woo, *J. Power Sources* 158 (2006) 1344.
- [6] R.R. Adžić, J.X. Wang, B.M. Ocko, J. McBreen, *Handbook of Fuel Cells, EXAFS, XANES, SXS*, John Wiley & Sons, 2010
- [7] Ch. Hartnig, I. Manke, J. Schloesser, Ph. Krüger, R. Kuhn, H. Riesemeier, K. Wippermann, J. Banhart, *Electrochem. Comm.* 11 (2009) 1559.
- [8] I. Manke, Ch. Hartnig, N. Kardjilov, H. Riesemeier, J. Goebbels, R. Kuhn, Ph. Krüger; J. Banhart, *Fuel Cells* 10 (2010) 26.
- [9] R. Thiedmann, Ch. Hartnig, I. Manke, V. Schmidt, W. Lehnert, *J. Electrochem. Soc.* 156, 11 (2009) 1339.